Journal of Colloid and Interface Science **227,** 282–290 (2000)
doi:10.1006/jcis.2000.6833, available online at http://www.idealibrary.com on IDEAL®

A New Method for the Characterization of Electrically Conducting Liquid Bridges

Margaritis Kostoglou* and Thodoris D. Karapantsios†,[1]

**Chemical Process Engineering Research Institute, P.O. Box 1517, 540 06 University City, Thessaloniki, Greece; and †Department of Mechanical & Industrial Engineering, University of Thessaly, Pedion Areos, GR-38334 Volos, Greece*

Received July 12, 1999; accepted March 13, 2000

An electrical conductance technique is employed in investigating the behavior of constant volume liquid bridges when their length is altered. The liquid bridges are edge-pinned between two vertical, identical rods with a variable separation distance. Rods of different radius, material, and edge geometry are examined as they play a role in the response of the system. It is shown that liquid bridge volume and rod radius are the parameters that mainly influence the conductance signal. A mathematical framework is developed for the identification of the geometrical characteristics of liquid bridges explicitly from conductance data. The role of gravity is discussed in both the experiments and the theoretical analysis. The theoretical predictions obtained show a close agreement with measurements.

Key Words: **liquid bridge; electrical conductivity; surface tension; contact angle.**

INTRODUCTION

Several methods have been employed in the past to register liquid bridge behavior (1). A major part of this literature is devoted to studying the force exerted by the liquid bridge to its supporting solid boundaries. However, it appears that force measurements suffer from inevitable stability problems that require excessively meticulous procedures and further filtering of the data. Particularly when working with solid spheres, buoyancy corrections may make force data reduction very cumbersome (2). Errors from these sources may be appreciable considering the very small size of the bridges.

Measurement of the effective electrical conductance of conducting liquid bridges appears to be a tempting option for accurately monitoring liquid bridge behavior. In order to do so, a modified version of an ac conductance technique, originally developed in (3) to study flow characteristics in thin liquid films, is employed here. In the present work, the alternating electric field is used just as a characterization means of the liquid bridge and clearly there is a relation with the direct electric fields which are used for the stabilization (with respect to Rayleigh instability) of dielectric liquid bridges (4). The technique is characterized by satisfactory accuracy and stability and is particularly sensitive to liquid bridge characteristics. Systems of conducting liquids may directly benefit from measurements by this technique, e.g., water/surfactant systems in tertiary oil recovery from porous media, adsorption hysteresis in porous adsorbents, and capillary evaporation/condensation (5). A major advantage is the simplicity and robustness that makes it applicable for quick *in situ* measurements. Another potential application may be the measurement of interfacial tension or contact angle of conducting liquids avoiding the time-consuming step of image processing the interfacial profiles (6).

Thus, the primary objective of this work is to assess a novel conductance technique as a potential tool for studying liquid bridges of electrically conducting fluids. In order to do so, reliable computational tools that relate the physical parameters of the problem with the electrical conductance are needed. A short review of theoretical studies concerning liquid bridge configurations relevant to that of the present work follows. The solution of the Young-Laplace equation for the determination of interfacial shape is the subject of many works. An early account is given in (7). Among the various bridge configurations, considerable attention has been given to the shape of liquid bridges between two spherical particles as a prototype for the study of phenomena (e.g., evaporation, condensation, and oil recovery) in porous media. Melrose (8) examined the shape of a liquid bridge between two contacting spheres for zero Bond number. Erle *et al.* (5) solved the same problem for zero contact angle and arbitrary distance between the spheres. These authors noted the existence of two mathematical solutions and gave an empirical conjecture for the selection of the physically realizable (stable) one. For the same problem De Bisschop and Rigole (9) gave a thermodynamic derivation of the Young-Laplace equation and proposed a relevant criterion for the selection of the stable solution. Unfortunately, they assumed an incorrect rupture criterion. Mazzone *et al.* (2) derived the correct rupture criterion and further employed it to show the influence of gravity to the rupture distance. Latter, Lian *et al.* (10) confirmed the rupture criterion of Mazzone *et al.* (2) showing that it is equivalent to a more fundamental criterion based on the surface free energy of the system. Recently, Simons *et al.* (11) derived approximate analytical relations for the rupture energy of a liquid bridge

[1] To whom correspondence should be addressed.

0021-9797/00 $35.00

between two spheres with respect to wet agglomeration in the gas phase.

As regards liquid bridges between plane surfaces, Fortes (12) studied them for restricted (rods) and infinite (with contact angle as parameter) surfaces and for zero Bond number. The study of these liquid bridges in a gravity field was made by Boucher and Evans (13) for restricted surfaces and by Boucher *et al.* (14) for infinite surfaces. Latter, a stability analysis (somewhat similar to that of Lian *et al.* (10) for the spheres problem) was given for the restricted surfaces problem and zero gravity by Boucher and Jones (15).

The structure of the present work is as follows: First, a theoretical analysis is presented where the computational procedures for the evaluation of liquid bridge shape and conductance value are analyzed. The description of the experimental setup and procedures comes next. Finally, theoretical and experimental results are compared to each other and are further discussed.

THEORY

Liquid Bridge Shape

Let R be the radius of the rods and D the distance between the rods (see Fig. 1). Then, the shape of the axisymmetric liquid bridge $Y(X)$ is given from the solution of the Young-Laplace equation (Y, X, and D are made dimensionless by division with R).

$$-\frac{d^2Y}{dX^2}\left(1+\left(\frac{dY}{dX}\right)^2\right)^{-3/2}+\frac{1}{Y}\left(1+\left(\frac{dY}{dX}\right)^2\right)^{-1/2} = H-\mathrm{Bo}X, \quad [1]$$

where the Bond number is defined as $\mathrm{Bo}=\rho g R^2/\gamma$ and ρ, γ are the density and surface tension of the liquid that constitutes the liquid bridge. H is twice the dimensionless mean curvature of the bridge at $X=0$ and it is useful in the evaluation of the force between the rods due to the existence of the liquid bridge. In the present work, where the evaluation of the above force is not needed, H is only a dummy parameter that must be adjusted in order to satisfy the boundary conditions of Eq. [1].

Although in some cases the above form of the Young-Laplace equation has been solved using a finite element method (16), it is generally known that the numerical solution of this form has several problems due to pronounced sensitivity to the numerical accuracy (17). For this reason a variable transformation is suggested which results to a system of ordinary differential equations with the arc length of the liquid bridge as the independent variable

$$\frac{d\Phi}{dS}=H-\mathrm{Bo}X-\frac{\sin(\Phi)}{Y} \quad [2a]$$

$$\frac{dY}{dS}=\cos(\Phi) \quad [2b]$$

$$\frac{dX}{dS}=\sin(\Phi), \quad [2c]$$

where S is the dimensionless arc length of the liquid profile from the point $(Y, 0)$ to the point (Y, X) and Φ is the angle between the profile and the horizontal. A further simplification is possible due to the fact that the total arc length of the liquid bridge is not a concern in the present work. By proper division between the equations the following simplified system with X as the independent variable arises

$$\frac{d\Phi}{dX}=\frac{H-\mathrm{Bo}X}{\sin(\Phi)}-\frac{1}{Y} \quad [3a]$$

$$\frac{dY}{dX}=\frac{1}{\tan(\Phi)}. \quad [3b]$$

The boundary conditions are $Y(0)=Y(D)=1$. The total volume of the liquid bridge (nondimensionalized with πR^3) is given as

$$V=\int_0^D Y^2(X)\,dX. \quad [4]$$

The above equation is written as a differential equation with respect to X and is added as a third equation to the system [3].

Usually, the above problem is solved in a indirect manner, i.e., assuming a value for H and for $\Phi(0)$ and integrating the resulting initial value problem for the shape of the liquid bridges, e.g., (12, 14). In this way, the distance D between rods can be found from the condition $Y(D)=1$ and the liquid volume from Eq. [4] and then a table of V, D, H, $\Phi(0)$ can be constructed for the evaluation of liquid bridge geometry. Another (semidirect) approach is to assume a value for H or $\Phi(0)$ and to find the other according to the requirement that V or D must have a specific value. In this scheme also, tables such as those of the previous case can be constructed. Several aspects of this method have been used in (2) (with Newton Raphson iterations) and (10) (with bisectional searching) for liquid bridges hanging between spherical particles. However, for extracting information from experimental data, a direct approach is necessary. In this case, the macroscopically measured parameters V and D are known and the liquid bridge shape must be determined in order to find the parameter (typically the Bond number) value that

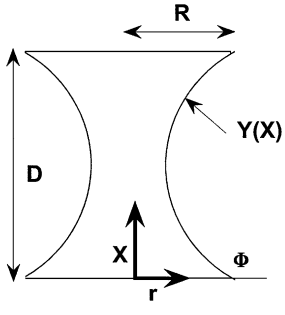

FIG. 1. Geometry of the liquid bridge.

matches the theoretical results with an independent experimentally measured quantity (e.g., electrical conductance or force between rods). This direct approach has been used in a closely related problem by Spencer *et al.* (18) who developed a method for the determination of interfacial tension from measurements of the force required to withdraw an axisymmetric solid body from a two-fluid interface contained in a cylindrical vessel. Their method for the solution of the problem is based on successive quadratic programming with the use of Lagrange multipliers to handle equality constraints.

In the present work a simple shooting method combined with an appropriately designed continuation procedure is used. The problem is to solve the system [3] with the respective boundary conditions and to find the value H that gives a specified liquid volume V. First, a value of H and $\Phi(0)$ is assumed and the initial value problem is integrated with the use of an explicit Runge Kutta integrator with self-adjusted step and prespecified accuracy (19) to find the $Y(D)$ and the V' value; the prime designates temporal values of the parameters. The Newton Raphson method with numerically computed derivatives is used for the correction of the H and $\Phi(0)$ values. The convergence has been achieved when $Y(D)=1$ and $V'=V$. So, in principle, for every pair of D and V values the liquid bridge shape can be computed by the above procedure. But in practice there are additional complexities. The equations, although they are not stiff, show an excessive parametric sensitivity with respect to H. This means that the solution of the Eqs. [3] can be quite different for almost identical values of H. A very clear example of parametric sensitivity of the Young-Laplace equation is given in Fig. 2 of (18). (The plots of Fig. 2 and Fig. 3 in the above paper are interchanged so Fig. 3 must be seen instead).

The existence of this parametric sensitivity means that a very good estimation of H is needed for the Newton Raphson method to converge. This problem is overcome by the use of a continuation approach. The method of continuation has also been used in (18). The complete procedure is as follows: For a given pair of values V and D and a given Bond number Bo, a cylindrical liquid bridge is assumed with $\mathrm{Bo}'=0$ and $D'=V$. It is important to note that for the existence of a stable cylindrical liquid bridge shape the Rayleigh criterion must be fulfilled. Having an exact solution (cylindrical shape with $\Phi(0)=\pi/2$ and $H=1$ for the zero Bond number) a zero order continuation procedure with respect to Bo′ is started. This means that the Bond number is increased and the initial values for the new Newton Raphson step are the converged values of the previous step. After the required Bond number Bo is reached, a new zero order continuation procedure with respect to D' from $D'=V$ to $D'=D$ is started. The above procedures are similar to the numerical integration of an initial value problem with Bo′ and D' as time-like variables, successively. The step size of D' must be very small in order to ensure convergence of the Newton Raphson method.

The above method ensures that from the two possible solutions the stable one is always taken. This can be demonstrated using the Fig. 7a of (12) which displays the possible configurations (with angle $\theta=\pi-\Phi(0)$) of liquid bridges for the present problem in V and D axis. Although that graph is for a zero Bond number, it is known that the general behavior is the same for finite Bond numbers (13). It is clear from the figure that for bridges with $\theta<\pi/2$ and D larger than a certain value there are two possible configurations of the bridge for every V, D pair from which only that of lower θ is stable. The continuation sequence starts from the diagonal of the above-mentioned figure first crosses the region of a unique solution and finally passes to the region of two possible configurations. This trajectory is a straight line parallel to the D axis. The parametric sensitivity that was previously mentioned ensures that the Newton Raphson method converges to the stable solution when passing from one region to the other since it is impossible to roll toward the unstable solution which has a clearly larger θ value. The continuation stops when the envelope curve (dot curve in Fig. 7a of (12)) is reached. At this point rupture of the liquid bridge occurs, $D=D_{\mathrm{rup}}$. Our code has been tested extensively to reproduce the results that are given in Fig. 7a of (12) for zero gravity conditions.

Conductivity Problem

If an electrical potential difference exists between the two rods the potential distribution in the liquid bridge is given by the solution of the following Laplace equation

$$\frac{1}{r}\frac{\partial}{\partial r}r\frac{\partial P}{\partial r}+\frac{\partial^2 P}{\partial X^2}=0 \quad \text{in } 0<r<Y(X) \text{ and } 0<X<D, \quad [5]$$

where P is the electrical potential normalized to be 1 at the one rod and 0 at the other.

The boundary conditions for the above equation are

$$P=1 \quad \text{for } X=0 \text{ and } 0<r<1 \quad [6a]$$

$$P=0 \quad \text{for } X=D \text{ and } 0<r<1 \quad [6b]$$

$$\left(\frac{\partial P}{\partial \vec{\mathbf{n}}}\right)_{r=Y(X)}=0, \quad [6c]$$

where $\vec{\mathbf{n}}$ is the unit normal vector.

Having the potential distribution, the dimensionless conductance K_{app} can be computed from the relation

$$K_{\mathrm{app}}=-2\pi\int_0^1\left(\frac{\partial P}{\partial X}\right)_{X=0} r\,dr. \quad [7]$$

The conductance is made nondimensionless with σR where σ is the specific conductivity of the liquid. The above mathematical problem is quite similar to the extensively studied problem of heat transfer in fins (20). Applying Green's theorem to a volume element (slice) of the liquid bridge between X and $X+\delta X$

results in

$$\int_{A(X+\delta X)} \frac{\partial P}{\partial X}\, dA - \int_{A(X)} \frac{\partial P}{\partial X}\, dA + \int_{A_s} \frac{\partial P}{\partial \vec{\mathbf{n}}}\, dA_s = 0, \qquad [8]$$

where $A(X) = \pi Y^2(X)$ is the cross-sectional area of the liquid bridge at position X and A_s is the external surface of the volume element. The third term of the equation can be set equal to zero due to the boundary condition [6c]. The average potential P_m over the cross section is defined as

$$P_m(X) = \frac{1}{A(X)} \int_{A(X)} P\, dA. \qquad [9]$$

Application of the Leibnitz rule to X cross section gives

$$\frac{d}{dX} \int_{A(X)} P\, dA = \int_{A(X)} \frac{\partial P}{\partial X}\, dA + \frac{dA}{dX} P(A_s, X). \qquad [10]$$

A similar equation is taken for $X + \delta X$ cross section. Up to this point no assumption has been made for the derivation of the descriptive equations and the function P is the one which results from the solution of Eq. [5]. Here, an assumption is introduced which considers that the function $A(X)$ is relatively smooth so the terms containing derivatives of $A(X)$ can be omitted in a first approximation. Using this assumption, Eqs. [8], [9], and [10] after some algebra give

$$A(X + \delta X) \frac{dP_m(X + \delta X)}{dX} - A(X) \frac{dP_m(X)}{dX} = 0. \qquad [11]$$

Finally, by dividing the above equation by δX and taking the limit $\delta X \to 0$, the following differential equation for $P_m(X)$ results

$$\frac{d}{dX} A(X) \frac{dP_m}{dX} = 0. \qquad [12]$$

This is just an approximation to Eq. [5] in the limit of small interface slope. The corresponding boundary conditions are $P_m(0) = 1$ and $P_m(D) = 0$ and the dimensionless conductance is given as $K_{app} = -\pi (dP_m/dX)_{X=0}$. Solution of Eq. [12] with its boundary conditions and substitution in the relation for K_{app} lead to the final result

$$K_{app} = \pi \left[\int_0^D Y^{-2}(X)\, dX \right]^{-1}. \qquad [13]$$

The integral is written in the form of a differential equation with respect to X and is added as a fourth equation in the system of [3] and [4]. The accuracy of Eq. [13] depends on the magnitude of the derivative dY/dX. This is typically small for liquid bridges with the exception of the highly disturbed bridges prior to their rupture. It is worth noting that the same Eq. [13] can be obtained in another way, as the zero order term of a singular perturbation expansion solution of Eq. [5] in rods with nonuniform cross section (21).

EXPERIMENTAL SETUP AND PROCEDURES

A small liquid bridge is formed between the tips of two equal solid rods, aligned vertically inside a temperature/humidity-regulated chamber to prevent evaporation. The upper rod is coupled with a precision cathetometer with a resolution of 5 μm/division. This cathetometer has a built-in threaded rotor on which the upper rod is firmly attached. When the threaded rotor rotates, the upper rod is made to rotate, this being converted to a linear displacement of the upper rod. The lower rod is permanently fixed underneath the upper rod.

An ultraprecision microsyringe is used to deposit the fluid that forms the liquid bridge. Uncertainty in withdrawing a reproducible amount of liquid from the microsyringe needle is a matter of concern, this effect being amplified on a percentage basis with smaller quantities of liquid. For the experiments performed in this study, the error in liquid volume determination is 1% at most.

The liquid used in this work was deaerated tap water, filtered mechanically to remove suspended particles larger than 1 μm. The water in the tests was kept at 25°C. Its specific conductivity was 720 μS/cm whereas its surface tension determined by both the Wilhelmy slide and the ring method measures 68 ± 0.2 mN/m.

Rods were constructed by either bronze or stainless steel, both excellent electrical conductors. The rods used in this study have radii 1.575 and 0.865 mm. The respective Bond numbers for the two rods are 0.36 and 0.11. Perhaps the major concern in such experiments is the construction of the tip of the rod to which the liquid bridge is anchored and which is deemed responsible for the stability of the three-phase contact line (22). The free end of the present rods is carefully machined to be a knife-edged circle. In addition, another pair of rods is constructed slightly tapered (9°) at the outside toward a tip radius of 0.865 mm. Electrical connection of the rotating upper rod is achieved by good contact of its free end with a special spring, in the form of a hard metal strip. The lower rod is connected through a normal lead wire.

Each experiment starts with initially forming a liquid bridge with a volume corresponding to a cylindrical shape if under no gravity conditions. This initial liquid bridge, distorted from the cylindrical shape by gravity, will be henceforth referred to as equivalent cylindrical bridge. Then, the separation of the bridge is increased first in linear steps of 250 or 100 μm, this being followed by gradually smaller steps down to 5 μm at the vicinity of bridge rupture. These initial large displacement steps of the upper rod ascertain good spreading of the liquid on the rods, being several times the full revolution of the cathetometer (50 μm). The mobility of the upper rod also serves to lead the foot of the liquid bridge (contact line) eventually to a position of minimum

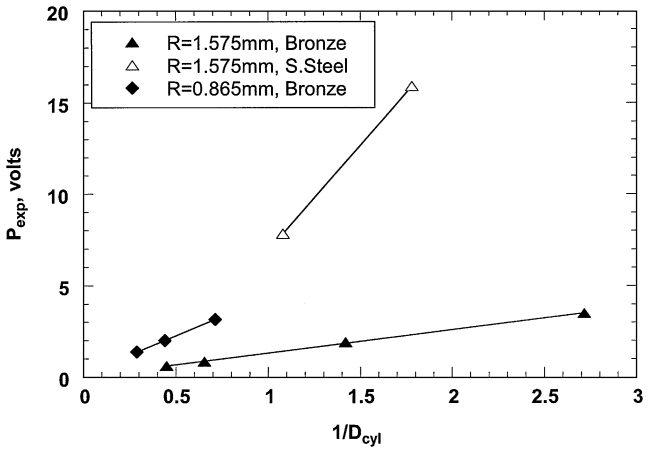

FIG. 2. Response of the technique for different rod radii and construction materials.

energy (23). In all our experiments the liquid bridge is assumed to remain attached to the solid rods at their circular edge. This is also manifested in the absence of hysteresis effects under different modes of executing the experiments, i.e., decreasing or increasing the separation of the bridge.

During the meniscus displacement the apparent electrical conductance of the bridges is recorded. The conductance probe comprises the two metallic rods serving as electrodes. An ac carrier voltage of 1.5 V (peak-to-peak) is applied across the probe at a frequency of 25 kHz in order to suppress undesirable electrode polarization and capacitive impedance. The response of the probe is fed to a special electronic analyzer, similar to that employed by Karapantsios and co-workers, (3, 24, 25). The analog dc voltage output of the analyzer is converted to equivalent conductance K_{app} of the medium between the electrodes using a calibration curve based on precision resistors. The output voltage is found to vary linearly with resistance in the entire range of resistors used. At least five runs are performed under all experimental conditions to check for repeatability and further increase the confidence of the calculated quantities.

Figure 2 shows the proportionality relation that holds between the as-measured voltage (and therefore electrical conductance) and the inverse dimensionless length of an equivalent cylindrical bridge for different diameters and construction materials of the rods. The larger the measured voltage the better in terms of recording it accurately whereas the larger the slope of the lines the higher the achieved sensitivity. Evidently, more accurate and sensitive measurements are made with smaller tip diameters. Moreover, stainless-steel rods improve substantially the performance of the technique in both accuracy and sensitivity. At first sight, this is rather surprising since bronze and stainless steel both have sizable electrical conductivities (26) and are highly wettable (22). A possible explanation may be sought in the varying chemical composition of the materials which may result in different surface inhomogeneities, surface quality upon machining (roughness and flaws), and different affinity to surface contamination (27) with concomitant influence on the passage of electric current. Analogous observations were previously made with respect to ring probes employed to measure the liquid holdup in packed beds and pipes (24). However, for data reduction purposes the experimentally determined conductance signal is normalized with respect to the corresponding equivalent liquid bridge conductance and these reduced quantities from either bronze or steel rods practically coincide.

RESULTS AND DISCUSSION

Theoretical Results

Some theoretical results for the behavior of the liquid bridges and their electrical conductance are presented in this section. In all cases it is assumed that the solid-liquid contact angle is smaller than $\Phi(0)$ so that detachment of the bridge from the rods does not happen. The values of V that are examined in the theoretical analysis are similar to the range used in the experiments. Figure 3 shows the dimensionless rupture distance D_{rup} as a function of Bond number at several dimensionless volume values. Apparently, this distance is quite insensitive to Bond number for small values of V. For larger values of V the rupture distance is a decreasing function of Bond number. As it can be seen in Fig. 3 the region of higher correlation between D_{rup} and Bo is for large V and small Bo. So, if an experimental procedure is to be developed for the evaluation of surface tension from measured rupture distances, the experimental parameters must be selected such that V is maximized (while taking care not to violate the Rayleigh stability criterion) and Bo is minimized.

Figure 4a displays the shape of liquid bridges with $V = 0.5$ and $\mathrm{Bo} = 0.5$ for several distance D values from $D = 0.5$ (equivalent cylindrical shape) to a distance prior to the rupture event. The vertical axis is not in the natural dimension X but in the normalized dimension X/D ($X/D = 0$ corresponds to the lower rod). For this small value of V and Bo the influence of gravity is small and the shape of liquid bridge is nearly symmetrical for small distance values and slightly asymmetrical for distance

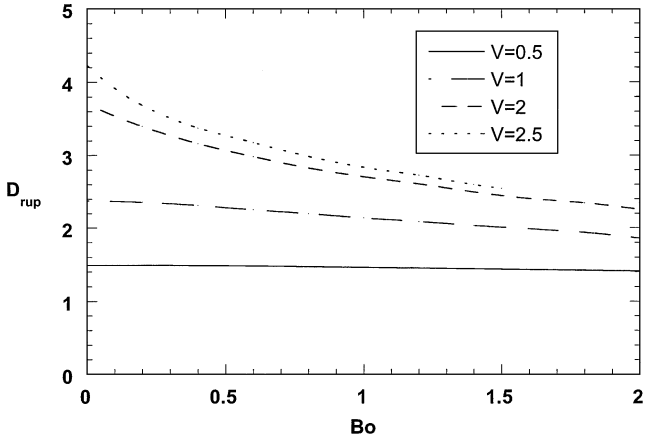

FIG. 3. Dimensionless rupture distance D_{rup} versus Bond number Bo for several values of the dimensionless volume V of the liquid bridge.

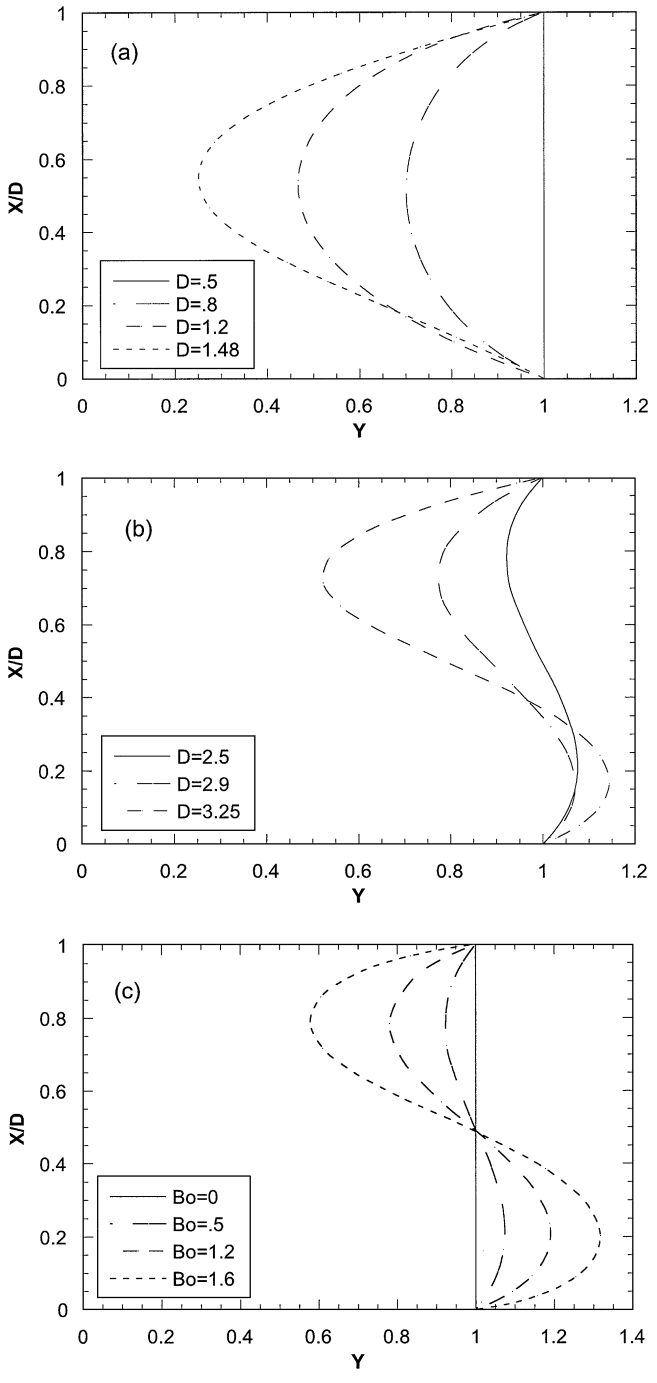

FIG. 4. Liquid bridge shape for (a) Bo = 0.5, $V = 0.5$; (b) Bo = 0.5, $V = 2.5$, and several dimensionless distance D values; and (c) $V = 2.5$, $D = 2.5$, and several Bond number values.

values close to D_{rup}. A very interesting observation is that the angle $\Phi(0)$ initially increases as D increases and after reaching a minimum it decreases until the rupture of the liquid bridge. A similar behavior of the so-called filling angle in the closely related problem of liquid bridges between spherical particles led De Bisschop and Rigole (9) to state that the rupture occurs at the minimum value of this angle. Later, it was proved theoretically and experimentally (2) that the above rupture criterion is not valid. Fig. 4b is similar to Fig. 4a but the volume of the liquid is now $V = 2.5$. Here the influence of gravity is obvious and the liquid bridge is quite asymmetrical with most of the liquid in the lower part of the bridge. By comparing Figs. 4a and 4b it is seen that the neck radius (minimum radius of the bridge) at the rupture point is larger when the influence of gravity is significant.

Figure 4c shows the shape of liquid bridges with $V = 2.5$ and $D = 2.5$ for several values of Bo. The cylindrical shape for Bo = 0 deforms more and more as the Bond number increases. It is noteworthy that all shapes take the value $Y = 1$ at almost the same X value (i.e., they have a common point). The departure of the liquid bridge from the cylindrical shape due to gravity can be also taken approximately in a closed form using a linear perturbation expansion with respect to Bond number (28).

Figure 5a shows the evolution of the effective electrical conductance of the bridge as the distance D increases for several values of V and Bo = 0.5. For ease in comparison, the results are given in a normalized form; both conductance and distance are normalized with respect to values for the equivalent cylindrical shape, K_{cyl} and D_{cyl}, where $D = \text{V}$. Curves of this type can be

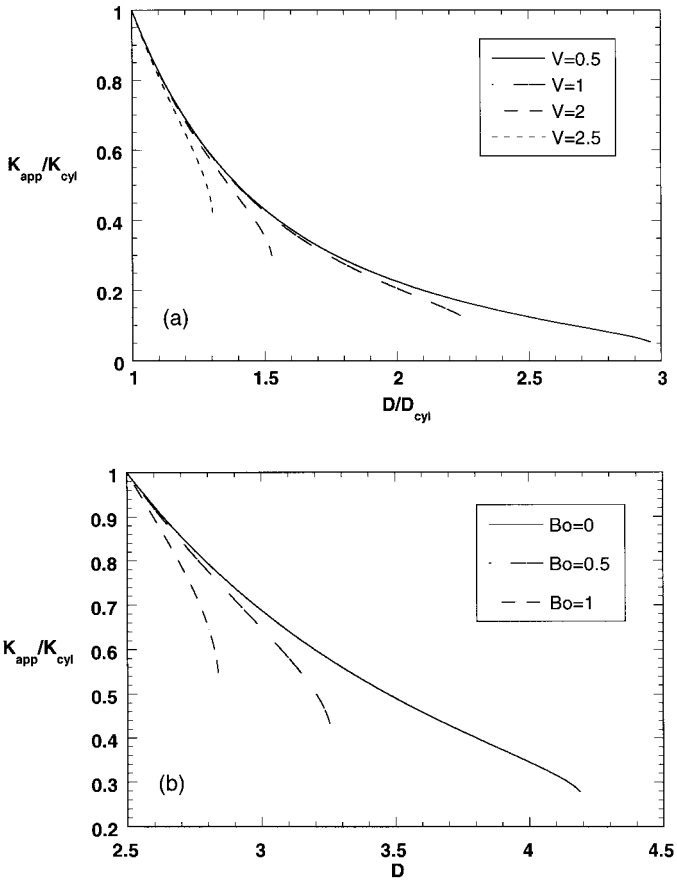

FIG. 5. Normalized conductance $K_{\text{app}}/K_{\text{cyl}}$ versus (a) normalized distance D/D_{cyl} for Bo = 0.5 and several values of V, (b) dimensionless distance D for $V = 2.5$ and several values of Bo.

obtained by direct use of the developed code since the trajectory of increasing D starting from the equivalent cylindrical shape is followed by the continuation sequence. It is obvious from Fig. 5a that as the volume of liquid decreases, the normalized conductance takes smaller values before the rupture occurs. Figure 5b shows the evolution of the dimensionless conductance with distance D for $V = 2.5$ and three values of Bond number. Here it is shown more clearly that for small Bond numbers there is a higher interrelation between Bond number and rupture distance. An important observation in both Figs. 5a and 5b is that in all cases the slope of the conductance versus D curves increases sharply prior to rupture, especially for high V values.

Experimental Results and Comparison with Predictions

When the separation of the solid rods is increased slowly at constant liquid bridge volume, the meniscus displaces until a certain critical bridge configuration is attained, at which stage the bridge becomes unstable and snaps. For small dimensionless volumes a nearly symmetric rupture is observed. In this case, the bridge neck remains at the mid-plane between the rods during the whole breakage sequence. For large volumes gravity dictates a nonsymmetric (but still axisymmetric) rupture as the bridge bulges and the neck sifts gradually upward until total disruption. Figure 6a shows the dimensionless rupture distance, D_{rup}, as a function of dimensionless liquid bridge volume, V, along with numerical predictions (theory). The agreement between data and predictions is excellent.

A very dramatic demonstration of gravity on liquid bridge characteristics is displayed in Fig. 6b. As the liquid volume increases beyond a certain value, the separation distance between the points of an equivalent cylindrical bridge and rupture gets drastically smaller. This behavior may impose an upper limit of easily reproducible data taken with the conductance technique as regards practical applications.

To present and compare the experimental data from various experiments, it is advisable to normalize the apparent conductance value at every separation of the bridge, K_{app}, with that corresponding to an initial equivalent cylindrical liquid bridge, K_{cyl}, in order to eliminate errors in liquid conductivity measurements. Figure 7 presents reduced conductance data, $K_{\text{app}}/K_{\text{cyl}}$, versus reduced separation distance, D, taken with two rods of different radius ($R = 1.575$ mm, Bo $= 0.36$, and $R = 0.865$ mm, Bo $= 0.11$) and various dimensionless liquid volumes. For small volumes, a steep decay is observed just after the departure from the equivalent cylindrical shape, being followed by a gradual decrease. For large volumes the trends are inversed. Yet, in all curves the vicinity of bridge rupture is characterized by an abrupt drop of the signal. It is apparent that the smaller the liquid volume the larger the overall drop in normalized conductance. Despite the difference in radii, comparable curves are obtained for similar bridge volumes regarding both curve decline and subsequent rupture point. This indicates the dominant effect of liquid volume on the response of the technique. The effect of gravity becomes more prominent as volume increases causing the bridge to snap at smaller departures from the equivalent cylindrical shape and, therefore, at relatively higher conductance values. This is in accord with the theoretical arguments advanced in Fig. 5a. The agreement between theoretical and experimental results in

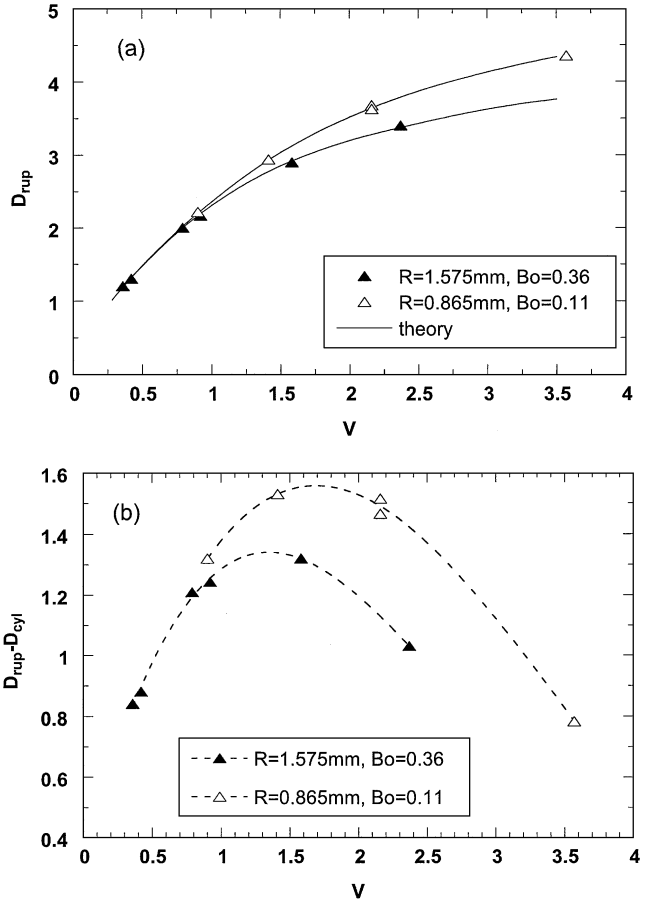

FIG. 6. (a) Dimensionless rupture distance, D_{rup}, and (b) dimensionless separation distance between points of rupture and equivalent cylindrical bridge, $D_{\text{rup}} - D_{\text{cyl}}$, versus dimensionless bridge volume V, for different rod radii.

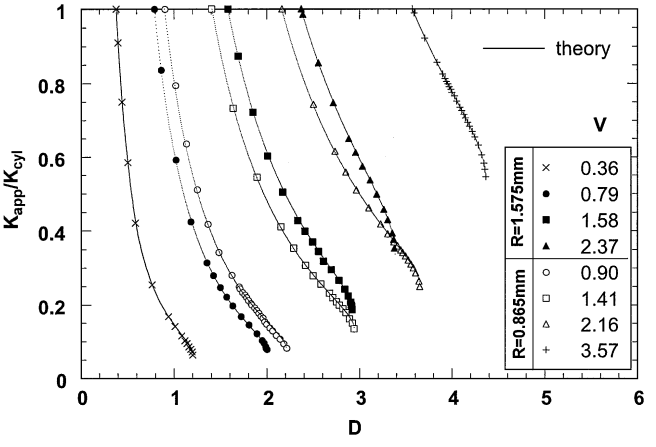

FIG. 7. Normalized apparent conductance signals $K_{\text{app}}/K_{\text{cyl}}$, versus dimensionless separation distance D, taken with rods of different radius ($R = 1.575$ mm, Bo $= 0.36$, $R = 0.865$ mm, Bo $= 0.11$).

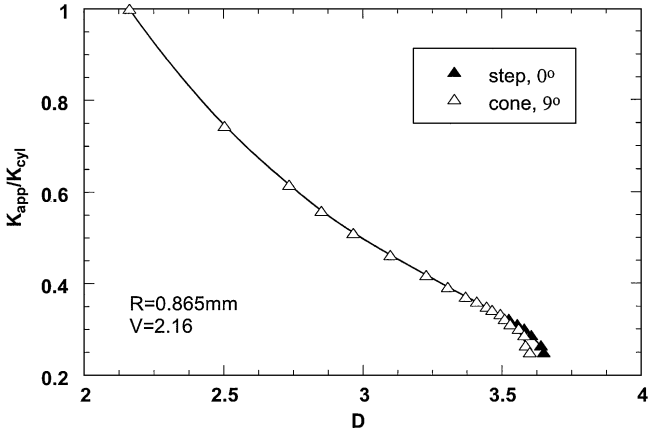

FIG. 8. Normalized apparent conductance signals, K_{app}/K_{cyl}, versus separation distance D, for rods of different tip characteristics ($R = 0.865$ mm, $V = 2.16$).

Fig. 7 is rather surprising taking into account the approximate character of Eq. [13]. This is mainly due to the scaling of the plot. In fact, the deviation between theory and experiment in the region close to rupture (where the maximum bridge distortion occurs) is up to 10%. This deviation reduces with increasing dimensionless volume V, as theory predicts, due to smoother bridge surfaces (Fig. 4b).

Experimental K_{app}/K_{cyl} versus D curves can be readily used to infer the value of liquid surface tension. Fitting the experimental curves with theoretical predictions for an appropriate Bond number can do this, if just V and R are known. For liquid bridges forming not between restricted rods but between infinite surfaces it is also possible to employ the same procedure to deduce the value of the contact angle between the liquid and the solid surface by using the corresponding liquid bridge descriptive equations (14). Work in that direction is under way.

The employed experimental parameters (rods radii and liquid medium) assure that no recession of the bridge contact line away from the edge of the rods is expected due to hydrodynamic instabilities (13). However, in a real system the interfacial stability limit may also be transgressed by violations of contact angle conditions such as minor construction imperfections, sharpness of the edge, or other geometrical peculiarities at a submicroscopic level (29). Tests performed with rods slightly tapered near the tip (9°; $R = 0.865$ mm) showed that, with bridges of relatively large volume, even moderate external vibrations of the setup could be responsible for slight movement of the contact line at the vicinity of bridge rupture since in this case gravity makes the bridge bulge excessively. Interestingly, the radial direction of overflow over the edge was random from run to run, suggesting that there were no preferential sites of instability around the edge. Figure 8 clearly demonstrates the influence of gravity which, at large separations of the rods, bulges the bridge to angles beyond Gibbs stability condition (29) and spills the liquid over the edge.

CONCLUSIONS

An electrical conductance technique is proposed as a potential tool for making accurate *in situ* identification of liquid bridges. The normalized conductance signal is influenced by both liquid bridge volume and rod diameter but is independent from rod construction material inasmuch as it is a good electrical conductor. Overall, the conductance data appear to be indicative of liquid bridge configuration. An integrated mathematical framework is proposed for the explicit evaluation of liquid bridge geometrical characteristics from conductance data under the influence of gravity. Data gathered in this work as regards rupture distance with respect to bridge volume agree favorably with theoretical predictions. It is apparent that by proper selection of rod geometrical characteristics, the surface tension of the conducting liquid bridge may be evaluated form the precise measurement of the separation distance of the bridge and the respective apparent conductance signal. Regarding potential practical applications, it might be useful to employ this conductance technique in order to examine the influence of surfactant systems on the behavior of conducting liquid bridges like those encountered in tertiary oil recovery or capillary evaporation/condensation.

ACKNOWLEDGMENT

The authors express their gratitude to Prof. A. J. Karabelas of the Department of Chemical Engineering of the Aristotle University of Thessaloniki for allowing the experiments described in this paper to be performed in his lab.

REFERENCES

1. Ratke, L., Walter, H., and Feuerbacher, B. (Eds), "Materials and Fluids Under Low Gravity," Lecture Notes in Physics, pp. 271, 323, 331. Springer-Verlag, Berlin, 1996.
2. Mazzone, D. N., Tardos, G.I., and Pfeffer, R., *J. Colloid Interphase Sci.* **113,** 544 (1986)
3. Karapantsios, T. D., Paras, S. V., and Karabelas, A. J., *Int. J. of Multiphase Flow* **15,** 1 (1989).
4. Gonzalez, H., Mc Cluskey, F. M. J., Castellanos, A., and Barrero, A., *J. Fluid Mech.* **206,** 545 (1989).
5. Erle, M. A., Dyson, D. C., and Morrow, N. R., *AIChE J.* **17,** 115 (1971).
6. Song, B., and Springer, J., *J. Colloid Interface Sci.* **184,** 64 (1996).
7. Padday, J. F., *Pure Appl. Chem.* **48,** 485 (1976).
8. Melrose, J. C., *AIChE J.* **12,** 986 (1966).
9. De Bisschop, F. R. E., and Rigole, W. J. L., *J. Colloid Interface Sci.* **88,** 117 (1982).
10. Lian, G., Thornton, C., and Adams, M. J., *J. Colloid Interface Sci.* **161,** 138 (1993).
11. Simons, S. J. R., Seville, J. P. K., and Adams, M. J., *Chem. Eng. Sci.* **49,** 2331 (1994).
12. Fortes, M. A., *J. Colloid Interface Sci.* **88,** 338 (1982).
13. Boucher, E. A., and Evans, M. J. B., *J. Colloid Interface Sci.* **75,** 409 (1980).
14. Boucher, E. A., Evans, M. J. B., and McGarry, S., *J. Colloid Interface Sci.* **89,** 154 (1982).
15. Boucher, E. A., and Jones, T. G. J., *J. Colloid Interface Sci.* **126,** 469 (1988).
16. Zasadzinski, J. A. N., Sweeney, J. B., Davis, H. T., and Scriven, L. E., *J. Colloid Interface Sci.* **119,** 108 (1987).

17. Pozrikidis, C., "Introduction to Theoretical and Computational Fluid Dynamics," p. 172. Oxford Univ. Press, New York, 1997.
18. Spencer, J. L., Gunde, R., and Hartland, S. *Comput. Chem. Eng.* **22,** 1129 (1998).
19. Press, W. H., Teukolsky, S. A., Vetterling, W. T., and Flannery, B. P., "Numerical Recipes. The Art of Scientific Computing," p. 704. Cambridge Univ. Press, New York, 1992.
20. Michailov, M. D., and Özisik, M. N., "Unified Analysis and Solutions of Heat and Mass Diffusion," p. 234. Wiley, New York, 1984.
21. Kevorkian, J., and Cole, J. D., "Multiple Scales and Singular Perturbation Methods," p. 182. Springer-Verlag, New York, 1996.
22. Adamson, A. W., "Physical Chemistry of Surfaces," p. 332. Wiley, New York, 1982.
23. Miller, C. A., and Neogi, P., "Interfacial Phenomena. Equilibrium and Dynamic Effects," p. 54. Decker, New York, 1985.
24. Tsochatzidis, N. A., Karapantsios, T. D., Kostoglou, M., and Karabelas, A. J., *Int. J. Multiphase Flow* **18,** 653 (1992).
25. Karapantsios, T. D., Tsochatzidis, N. A., and Karabelas, A. J., *Chem. Eng. Sci.* **48,** 1427 (1993).
26. Perry, R. H., and Green, D. W., "Chemical Engineer's Handbook," Chap. 23. McGraw-Hill, New York, 1997.
27. White, M. L., *in* "Clean Surfaces, Their Preparation and Characterization for Interfacial Studies" (G. Goldfinger, Ed). Decker, New York, 1970.
28. Sanz, A., and Martinez, I., *J. Colloid Interface Sci.* **93,** 235 (1983).
29. Oliver, J. F., Huh, C., and Mason, S. G., *J. Colloid Interface Sci.* **59,** 568 (1977).